AD-A073 079 ROME AIR DEVELOPMENT CENTER GRIFFISS AFB NY F/G 17/1
HEMISPHERICAL COVERAGE OF FOUR-FACED AIRCRAFT ARRAYS.(U)
MAY 79 R J MAILLOUX, W G MAVROIDES

UNCLASSIFIED RADC-TR-79-176 NL


1·0
1·1
1·25
2·8
3·15
3·5
4·0
4·5
1·4
2·5
2·2
2·0
1·8
1·6
NATIONAL BUREAU OF STANDARDS

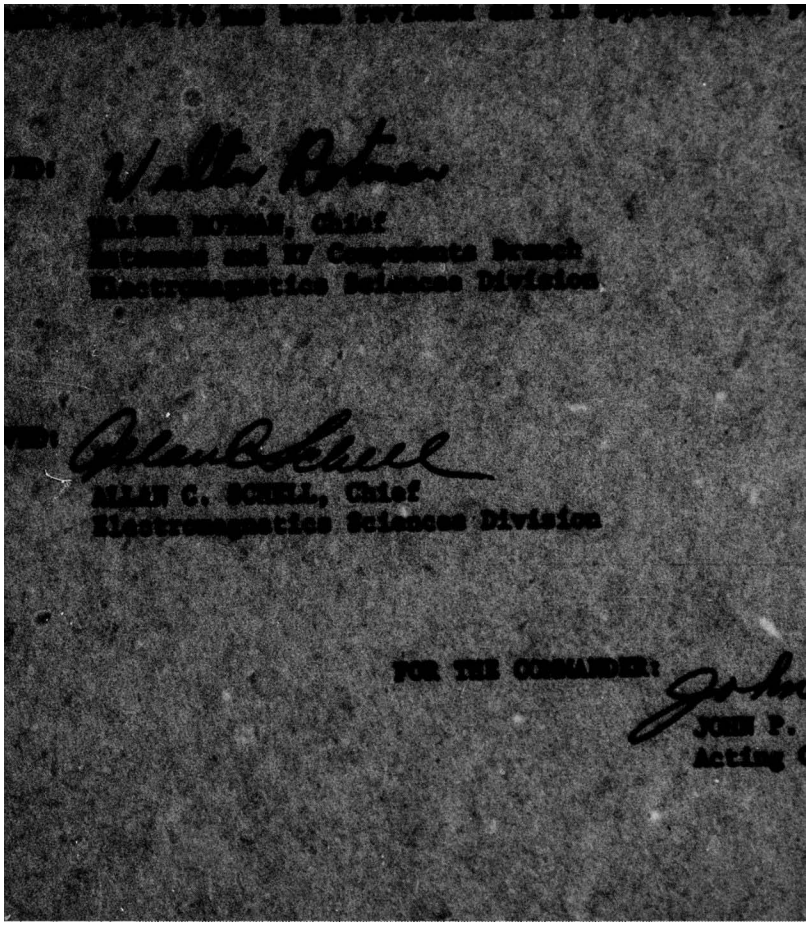

Unclassified

SECURITY CLASSIFICATION OF THIS PAGE (When Data Entered)

REPORT DOCUMENTATION PAGE	READ INSTRUCTIONS BEFORE COMPLETING FORM
1. REPORT NUMBER (14) RADC-TR-79-176	2. GOVT ACCESSION NO. (9)
4. TITLE (and Subtitle) (6) HEMISPHERICAL COVERAGE OF FOUR-FACED AIRCRAFT ARRAYS.	5. TYPE OF REPORT & PERIOD COVERED In-House Report Apr 78 - Apr 79
	6. PERFORMING ORG. REPORT NUMBER N/A
7. AUTHOR(s) (10) Robert J. Mailloux, William G. Mavroides	8. CONTRACT OR GRANT NUMBER(s) N/A
9. PERFORMING ORGANIZATION NAME AND ADDRESS Deputy for Electronic Technology (RADC/EEA) Hanscom AFB Massachusetts 01731	10. PROGRAM ELEMENT, PROJECT, TASK AREA & WORK UNIT NUMBERS 62702F 46001402 (16)
11. CONTROLLING OFFICE NAME AND ADDRESS Deputy for Electronic Technology (RADC/EEA) Hanscom AFB Massachusetts 01731 (11)	12. REPORT DATE May 1979
	13. NUMBER OF PAGES 18
14. MONITORING AGENCY NAME & ADDRESS(if different from Controlling Office) (12) 19p.	15. SECURITY CLASS. (of this report) Unclassified
	15a. DECLASSIFICATION/DOWNGRADING SCHEDULE N/A

16. DISTRIBUTION STATEMENT (of this Report)

Approved for public release; distribution unlimited.

17. DISTRIBUTION STATEMENT (of the abstract entered in Block 20, if different from Report)

18. SUPPLEMENTARY NOTES

19. KEY WORDS (Continue on reverse side if necessary and identify by block number)

Aircraft arrays
Phased arrays
Communication arrays

20. ABSTRACT (Continue on reverse side if necessary and identify by block number)

This report describes the radiating characteristics of a four-faced array with faces arranged in a streamlined configuration for hemispherical coverage. The report presents new experimental and theoretical results giving coverage for a side array in the plane perpendicular to the cylinder and shows that the structure radiates both polarizations efficiently for angles from the zenith to the horizon. In the absence of mutual coupling effects, the circularly polarized radiation remains within approximately 1 dB of the array projection factor.

DD FORM 1 JAN 73 1473 EDITION OF 1 NOV 65 IS OBSOLETE

Unclassified

SECURITY CLASSIFICATION OF THIS PAGE (When Data Entered)

next page

309 050

gm

20. Abstract (Continued)

Finally the report presents coverage contours for a four-faced array with the front and back faces half the size of the side faces. In this case, the proper choice of front array tilt angle can result in a hemispherical gain projection factor within 3.5 dB of peak gain over nearly the whole hemisphere.

Contents

Illustrations

Hemispherical Coverage of Four-Faced Aircraft Arrays

1. INTRODUCTION

One of the more persistent technological problems of aircraft satellite communications terminals is the need for flush-mounted or conformal SHF aircraft antennas with adequate coverage for communication over the entire upper hemisphere. Present aircraft Satcom antennas at SHF and higher frequencies are reflectors with over 30-dB gain, although one x-band experimental terminal has been developed (Maune[1]) with a low-profile, "hybrid" array that rotates in the axial plane and has electronic scanning in elevation. The difficulty with any such planar antenna is that the gain degrades so severely in scanning from zenith to horizon that the antenna aperture must be made far larger than that required by zenith gain constraints. This scanning loss for communication with a circularly polarized satellite antenna is due to a combination of effects. Among these are array element mutual coupling that results in reflection losses, the reduction in directivity associated with the reduced array projection near the horizon, the loss due to diffraction around the aircraft's locally cylindrical surface, and a 3-dB polarization loss if the aircraft antenna is linearly polarized. These physical

---

(Received for publication 6 June 1979)

1. Maune, J.J. (1972) An SHF Airborne Receiving Antenna, Twenty-Second Annual Symposium on USAF Antenna Research and Development.

limitations are described in an earlier reference (Mailloux[2]). Taken together they require that for a given horizon gain in the neighborhood of 20 dB for a square array and in the absence of circuit losses, one must provide an additional 12 to 14 dB of area gain. Adding three 3 dB for circuit losses leads to the conclusion that to provide 20 dB of gain over the upper hemisphere with a hybrid mechanical and phase-scanned, flush-mounted antenna, one must use an antenna area with equivalent directivity of approximately 35 to 37 dB. Providing the same gain with a completely phase-scanned array would require an additional 3 dB of gain to overcome polarization loss. Surface wave techniques can provide gain at the 20-dB level for more efficiency (Mailloux[2]), but these techniques are restricted to less than 10 percent bandwidth.

The present study was undertaken to provide data describing the use of a four-faced array made up of two 45° faces oriented along the aircraft axis and smaller arrays for nose and tail coverage as shown in Figure 1. The goal of the project was to make two concessions at the outset and then to try to optimize performance. The concessions were to abandon the requirement for a flush-mounted array while substituting a narrow, streamlined radome, and to accept reduced gain, if necessary, in the conical regions near the nose and tail of the aircraft because of the use of smaller arrays in those directions as would be consistent with the streamlined shape shown in Figure 1.

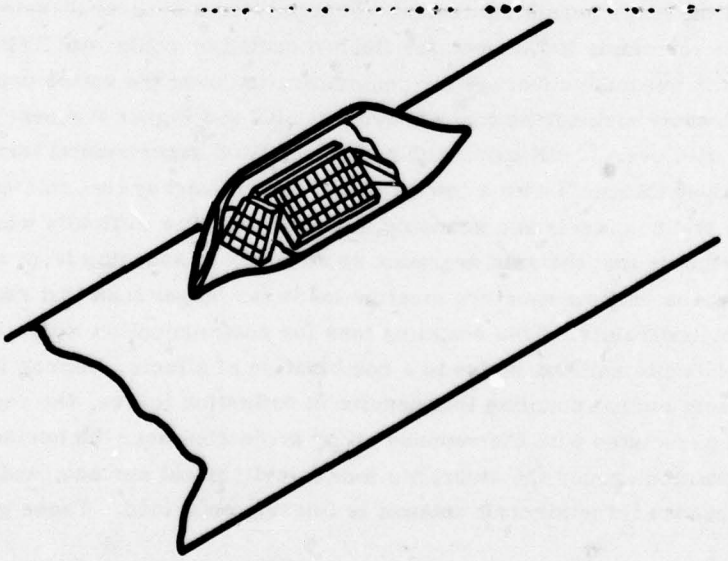

Figure 1. Four-Faced Tent Configuration

2. Mailloux, R.J. (1977) Phased array aircraft antennas for satellite communications, Microwave Journal 20(No. 10):38-42.

2. RADIATION CHARACTERISTICS OF THE FOUR-FACED ARRAY

An analytical/experimental study has been conducted to investigate the scanning properties of an array mounted at 45° from the horizontal at the top surface of an aircraft cylinder. The experimental part of the program used a 64-element linearly polarized waveguide array scanned in the plane perpendicular to the aircraft axis, and mounted on an 8-foot by 12-foot ground screen section with an 84-inch radius of curvature. The array and ground plane are shown in Figure 2. The array consists of eight rows of eight elements each. Each row is 0.402 λ high at 9.5 GHz, and the peak of the array is 2.01 λ high. The patterns were computed by geometrical optics, and the basic equations are summarized in Appendix A. Figure 3 shows the measured and calculated E-plane radiation patterns for the array scanned to three different elevation angles: zenith, 45°, and horizon. In all cases the theoretical data give an excellent representation of the experimental scan behaviour. Figure 4 shows the gain vs scan characteristics for axial (H-plane) and radial (E-plane) polarizations for an array of square waveguide apertures 0.4 λ on a side as the array is scanned from zenith to horizon.

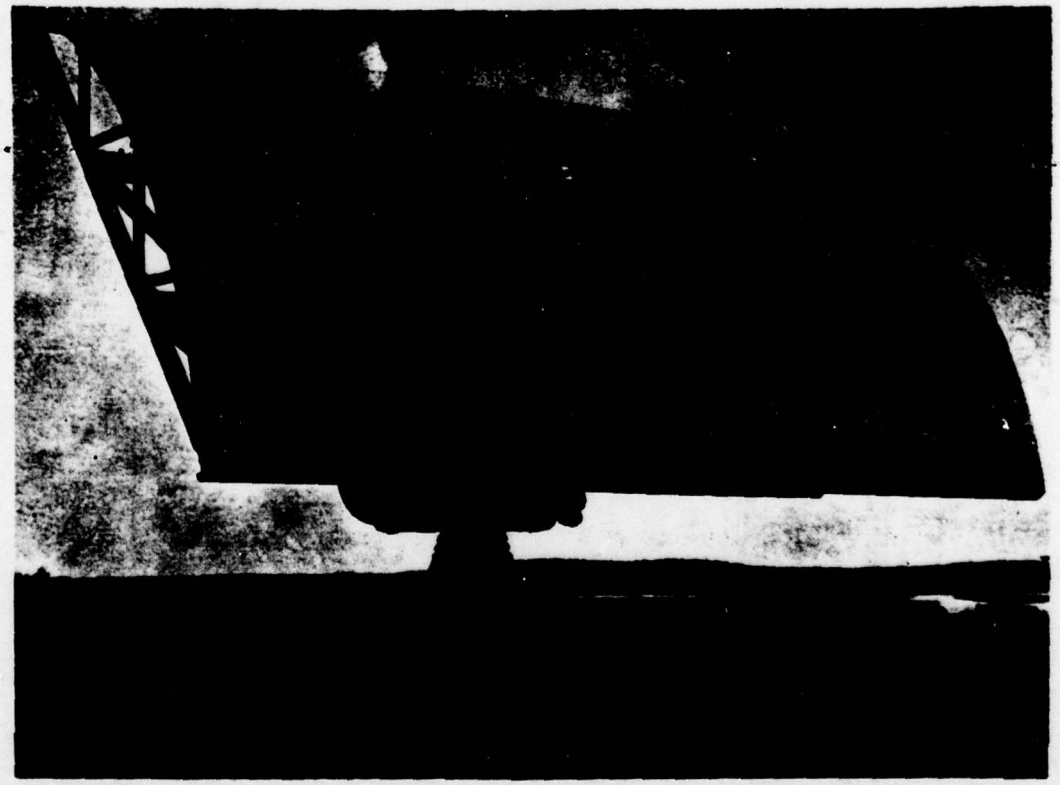

Figure 2. Experimental Array and Ground Plane

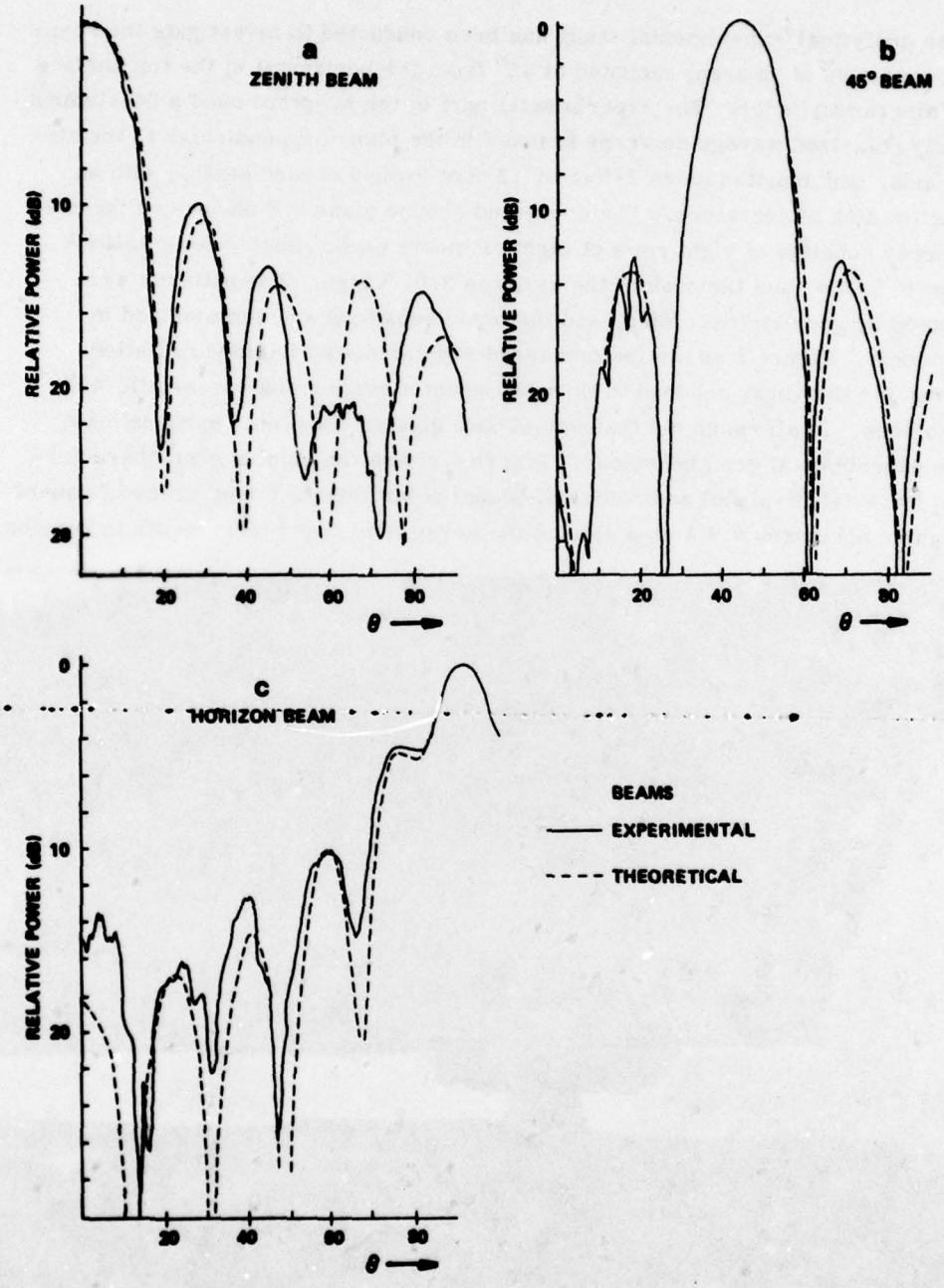

Figure 3. Experimental and Theoretical Radiation Patterns

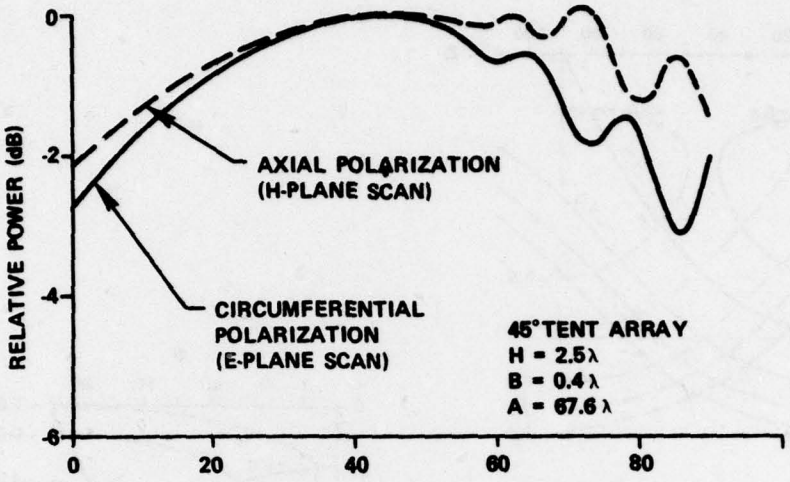

Figure 4. Gain vs Scan Characteristics for Axial and Circumferential Polarization

The radiation at angles less than 45° from zenith are free from specular reflections, and so the exhibited gain falloff in that region is just the array element pattern here approximated by the product of the projection factor $\sqrt{\cos(\theta - 45^{\circ})}$ and the pattern of an isolated element. The total degradation at zenith is about 2.1 dB for the H-plane elements and about 2.7 dB for the E-plane. If the array were excited with circular polarization, the gain reduction at zenith into a circularly polarized satellite antenna would thus be about 2.4 dB (or only 0.9 dB in excess of the 1.5 dB projection factor). Nearer the horizon, both patterns show the effect of specular reflection from the curved ground plane, but the ripples introduce deviations of at most 1 dB from the pattern without reflections. Moreover, there is enough gain due to the image near the horizon that the actual loss in gain, relative to circularly polarized satellite, is never more than about 1.9 dB (at 85°). This is somewhat of an improvement as compared with the pattern coverage near zenith where there are no reflections.

In summary, this data suggests that the gain to a circularly polarized receiving antenna can be within about 1 dB of the cos (θ - 45°) projection factor for an array inclined 45° mounted on a conducting cylinder.

Figure 5 shows the scan contours, sometimes called "scanning shields," for two arrays mounted as in Figure 1 for the case in which the front array has 3 dB less gains than a side array. Figure 5 shows projection factors as computed in Appendix B, and does not include the effects of array mutual coupling or the actual

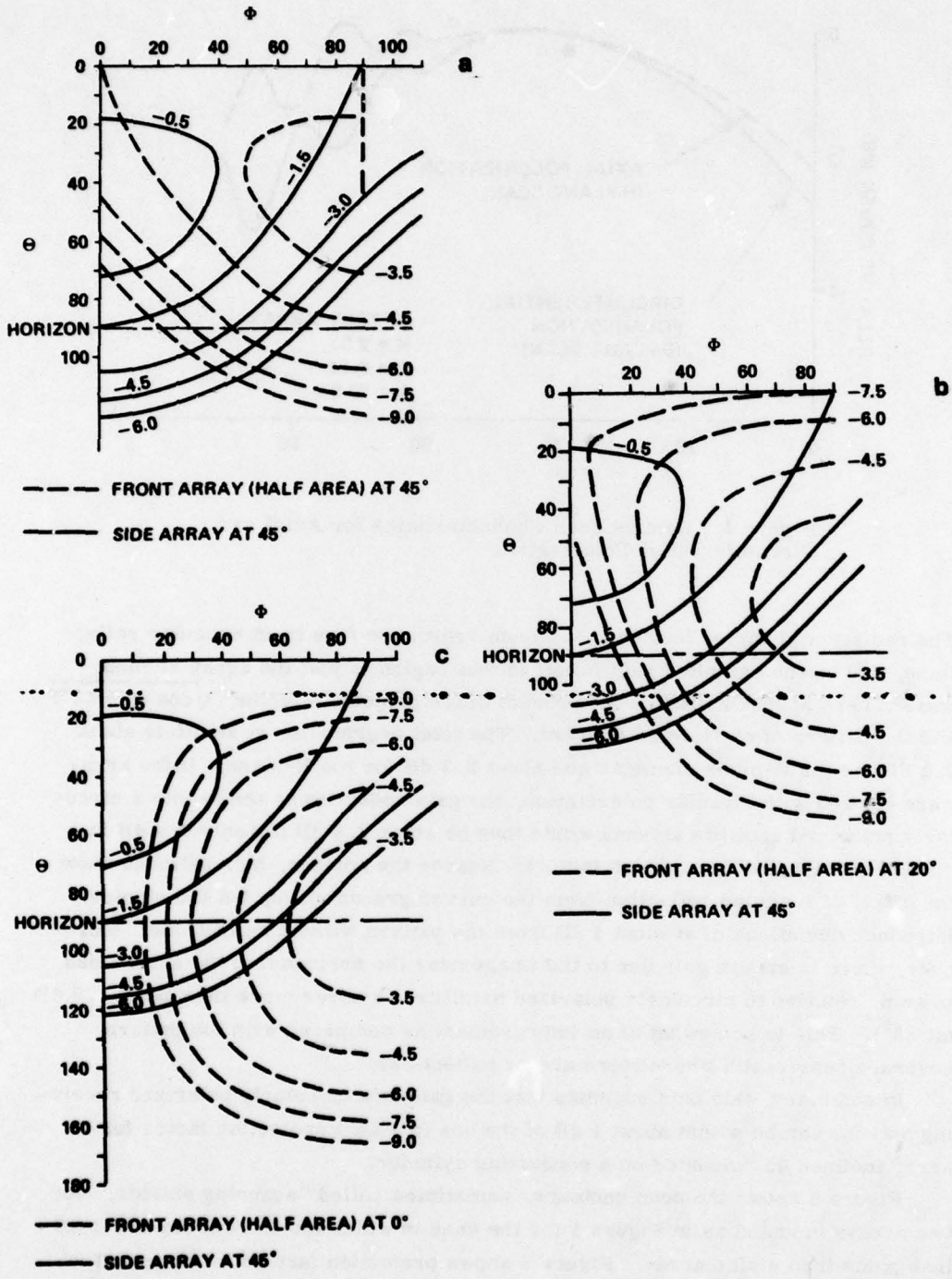

Figure 5. Hemispherical Coverage Contours

element patterns. As indicated above, element patterns can be expected to reduce the gain to a circularly polarized source by about another 1 dB. The side array data is shown solid, and the front array dashed. Figure 5a shows the scan coverage for two arrays mounted at 45°, and indicates that this selection leads to only one small area near the horizon with projection factor less than -4.5 dB relative to the peak gain of the side array. Figure 5b shows the scan characteristics that result when the front array is mounted at 20° from the vertical. This configuration offers good coverage near the horizon, with minimum hemispherical projection factor about 4 dB below the peak gain of the larger (side) array except in a very small region near the horizon. Figure 5c shows the scan shield for the front array at 0° (vertical). This configuration optimizes the horizon coverage, and has a projection factor over the hemisphere within 3.5 dB of the peak. Relating the projection factor to gain results in about 4.5 dB maximum gain reduction over the hemisphere. These data indicate that if good coverage at the horizon is a premium, then a nearly optimum solution has the side arrays at 45° and the front and back arrays nearly vertical. However, for any given tent cross section, it may be advantageous to tilt the front and back arrays to a 45° angle as well as the side arrays. This results in approximately 1.5 dB more available area gain, because a larger array can fit into the same space. Although this configuration provides little or no added gain at the horizon as compared with the smaller vertical array, it does offer increased gain throughout most of the hemisphere, and it utilizes the available space in a more efficient manner at the expense of requiring more array elements.

3. CONCLUSION

These experimental and theoretical results lead to the conclusion that it is possible to construct a four-faced array over a conducting cylinder and provide circularly polarized radiation and gain within about 4.5 dB of the peak gain for the larger side arrays. The analysis takes minimal account of mutual coupling effects by assuming an effective element pattern for the array elements that is the product of the projection factor and isolated element pattern.

Adding roughly 3 dB for feed and phase shifter losses leads to the combination of two side arrays with roughly 28 dB directivity and front and rear arrays with 25 dB directivity in order to provide 20 dB gain over the hemisphere.

Although requiring more phase controls than a hybrid mechanical/electronic array, the four-faced geometry has fully electronic scan, has much wider bandwidth, has a smaller array configuration that requires no large hole in the aircraft, and is potentially a light-weight, low-drag candidate SHF aircraft array.

Appendix A

Geometrical Optics Expressions for Radiation of an Element Above a Conducting Cylinder

Figure A1 shows the geometry of an array element mounted above a conducting cylinder of radius a. The element is in an array whose normal is tilted an angle ζ from the zenith. The peak of the array is a height H from the top of the cylinder. The equations given here are a special case of those given by Kouyoumjian and Pathak[3] and describe the spectral radiation in the plane normal to the cylinder.

The radiated field at p(x, y) for a source at x', y' with polarization vector $\hat{\eta}$ is given by the expression

$$E = E^i(P) + \bar{R} \cdot E^i(Q_R)\, e^{-jk_o S}\, g$$

where

$$E^i(P) = \frac{e^{-jk_o R_o}}{R_o}\, \hat{\eta}\, f(\theta)$$

---

3. Kouyoumjian, R. G. and Pathak, P. H. (1974) A uniform geometrical theory of diffraction for an edge in a perfectly conducting surface, Proc. of the IEEE 62(No. 11):1448-1461.

and

$$E^i(Q_R) = \frac{e^{-jk_o R_{inc}}}{R_{inc}} \hat{\eta}\, f(\theta_1)$$

Here θ_1 is the angle between the source at (x', y') and the point of specular reflection $Q_R(X_o, Y_o)$, and R_{inc} is the distance between the source point and the point Q_R, and is

$$R_{inc} = \sqrt{(x' - x_o)^2 + (y' - y_o)^2}$$

R_o is the distance from the source to point P (x, y)

$$R_o = \sqrt{(x - x')^2 + (y - y')^2}$$

The distance S is measured from the reflection point Q_R and the observation point p, and is given by

$$S = R_o - R_{inc} \cos(\theta_1 - 0)$$

The function $f(\theta)$ is the element pattern for a source in the array, and is here approximated by

$$f(\theta) = e(\theta) \sqrt{\cos(\theta - \zeta)}$$

for $e(\theta)$ the element pattern of an isolated source.

The dyadic reflection coefficient $\overline{R}$ for the case of a circular cylinder with no radial variation is given by

$$\overline{R} = \begin{bmatrix} 1 & 0 \\ 0 & -1 \end{bmatrix} = \hat{\theta}\,\hat{\theta} - \hat{z}\,\hat{z}$$

Under normal incidence the polarization unit vector $\hat{\eta}$ is $\hat{z}$ for axial polarization and $\hat{\theta}$ for radial polarization.

The coefficient g is given by:

$$g = \sqrt{\frac{\rho_1^r \rho_2^r}{(\rho_1^r + S)(\rho_2^r + S)}}$$

where the parameters ρ_1^r and ρ_2^r are the principal radii of curvature of the reflected wave at Q_R in the plane of incidence and normal to the plane of incidence, so that

$$\rho_2^r = R_{inc}$$

and

$$\frac{1}{\rho_1^r} = \frac{1}{R_{inc}} + \frac{2}{a \cos(\pi/2 - \alpha)}$$

where α is the angle between the reflected ray at the point Q_R and the tangent to the cylinder at Q_R. The angle is obtained using Snells Law to find the specular reflection point that gives a reflected ray at the angle θ.

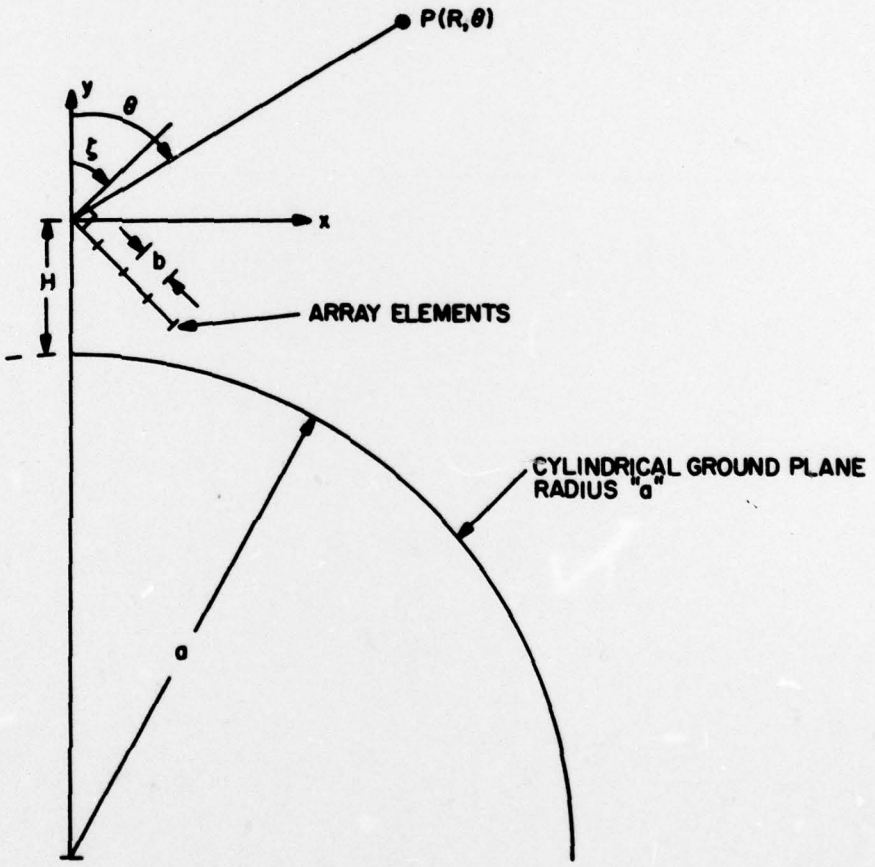

Figure A1. Array Geometry and Coordinates

The final expression for radiated field at P(x, y) is:

$$E = \frac{e^{-jk_o R_o}}{R_o} \left[\hat{\eta}\, f(\theta) + \overline{R} \cdot \hat{\eta}\, f(\theta_1)\, e^{-jk_o R_{inc}(1-\cos(\theta_1-\theta))} \cdot \left(\frac{R_o g}{R_{inc}} \right) \right]$$

Appendix B

Equations for Computing Scan Shields

Figure B1 shows the geometry of an array lying in the x-y plane, which is rotated about the x-axis by the angle δ relative to the system x', y', z'.

Conventional direction cosines w and v are defined relative to the unprimed (array) coordinate system

$$x = r \sin \theta \cos \phi = ru$$

$$y = r \sin \theta \sin \phi = rv$$

$$z = r \cos \theta = rc$$

An observation point specified by the direction cosines corresponds to the following Θ, Φ coordinates in the primed system:

$$\Theta = \cos^{-1} [v \cos \delta + c \sin \delta]$$

$$\Phi = \tan^{-1} \left[\frac{u}{- v \sin \delta + c \cos \delta} \right]$$

The array projection factor c determines the loss indicated on the scan shield diagrams according to the relation

$$\frac{P}{P_o} = 10 \log_{10} c$$

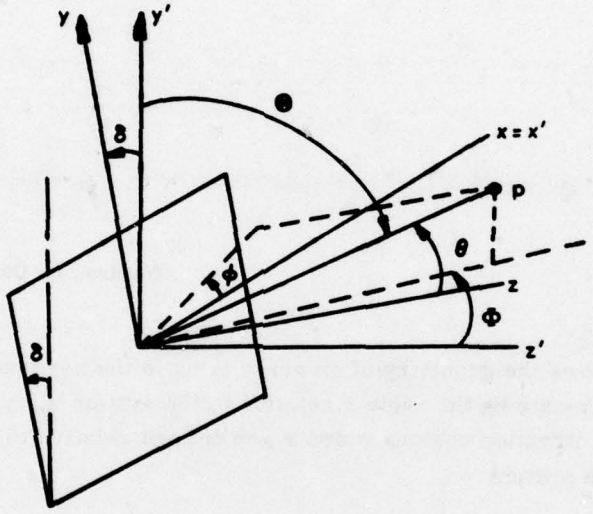

Figure B1. Coordinate Relationships for the Tilted Array